

Exchange bias of spin valve structure with a top-pinned $\text{Co}_{40}\text{Fe}_{40}\text{B}_{20}/\text{IrMn}$

C. Y. You,^{1,a)} H. S. Goripati,² T. Furubayashi,¹ Y. K. Takahashi,¹ and K. Hono^{1,2}

¹National Institute for Materials Science, 1-2-1 Sengen, Tsukuba 305-0047, Japan

²Graduate School of Pure and Applied Sciences, University of Tsukuba, Tsukuba 305-8571 Japan

(Received 23 April 2008; accepted 19 June 2008; published online 7 July 2008)

We have investigated the exchange bias of a directly top-pinned $\text{Co}_{40}\text{Fe}_{40}\text{B}_{20}/\text{IrMn}$ structure. An exchange bias was realized on the as-deposited samples, in which $\text{Co}_{40}\text{Fe}_{40}\text{B}_{20}$ exhibits a fully amorphous structure. A current-in-plane giant magnetoresistance effect was demonstrated on simple Ru/CoFeB/Cu/CoFeB/IrMn/Ru stacks prior to and after annealing. The amorphous CoFeB layer partially crystallized from the interface with a Cu spacer layer after annealed at 280 °C. © 2008 American Institute of Physics. [DOI: 10.1063/1.2956680]

Giant magnetoresistance (GMR) devices are widely used in read heads of ultrahigh density magnetic recording systems and magnetic sensors. In particular, current-perpendicular-to-plane (CPP) GMR has great potentials for future high-data-rate magnetic recording applications because of their low area resistance product (RA) which ranges from several tens of $\text{m}\Omega \mu\text{m}^2$ to several hundreds of $\text{m}\Omega \mu\text{m}^2$.^{1,2} Usually, a CPP-GMR spin valve consists of a free magnetic layer, a spacer layer, a pinned magnetic layer, and an antiferromagnetic pinning layer, typically IrMn or PtMn. Although the pinning layer is critical to the spin valve device, it does not contribute directly to the magnetoresistance (MR) signal; rather it constitutes a “parasitic” resistance of being similar to, or greater than, the total resistance of the active part of the spin valve structure, and significantly weakens the overall signal. Several methods have been used to weaken the effect of “parasitic” resistance. A current-confined-path structure made of a nano-oxide layer with small metallic channels has been proposed and confirmed to increase the MR ratio.^{3–5} Magnetic materials with large resistivity such as Co–Fe–Al and Co–Mn–Al have been used to produce a much larger output [ΔRA , change in area resistance product (RA)], 7.7 $\text{m}\Omega \mu\text{m}^2$ for Co–Fe–Al and 5.8 $\text{m}\Omega \mu\text{m}^2$ for Co–Mn–Al compared to 1.8 $\text{m}\Omega \mu\text{m}^2$ for CoFe.^{6,7}

Amorphous materials such as the CoFeB alloy are also promising candidates for the sense layers in practical GMR sensors, because of their high resistivity and low anisotropy, which could result in a higher sensitivity. Moreover, amorphous (hereafter a) $\text{Co}_{40}\text{Fe}_{40}\text{B}_{20}$ have been reported to possess a higher spin polarization of $\sim 63\%$ compared to $\sim 45\%$ for Co and $\sim 43\%$ for Fe deduced from point contact Andreev reflection (PCAR) measurements,⁸ and $\sim 58\%$ compared to $\sim 50\%$ for CoFe deduced from tunneling magnetoresistance ratio.^{9,10} The large spin asymmetry of the electronic transport in CoFeB is expected to be helpful for achieving a higher GMR effect. Note that the value of spin polarization of CoFeB measured by PCAR is close to or even higher than those reported for Heusler alloys, e.g., 0.62 for Co_2CrAl .¹¹ Heusler alloys require high temperature annealing for $L2_1$ or $B2$ ordering [>500 °C (Ref. 11)], which would limit their application as a top electrode in GMR de-

vices due to the low temperature tolerance of the spacer layer and Mn diffusion at high temperature.

A MR effect has been reported on a sandwich structure $\text{Co}_{72}\text{Fe}_8\text{B}_{20}/\text{Cu}/\text{Co}$ or $\text{Co}_{72}\text{Fe}_8\text{B}_{20}$ coupled by a NiO layer.^{12,13} However, exchange bias cannot be obtained from a directly top-pinned $a\text{-Co}_{72}\text{Fe}_8\text{B}_{20}$ or $\text{Co}_{60}\text{Fe}_{20}\text{B}_{20}/\text{IrMn}$ or FeMn structure at room temperature as reported in literatures,^{14–17} which would definitely restrict the applications of $a\text{-CoFeB}$ alloys in some of the spin valve structures such as the magnetic sensor and the dual spin valve. On the other hand, the application of the amorphous ferromagnetic layer would weaken the effect of lattice mismatching between the crystalline ferromagnetic layer and the spacer layer due to the less structural defects of interface between the amorphous ferromagnetic layer and the spacer layer. Therefore, investigating the exchange bias of a top-pinned $a\text{-CoFeB}/\text{IrMn}$ or FeMn structure for a different composition may be worthwhile. The first important step for the above subject would be to demonstrate the exchange bias and the antiparallel magnetic configuration between the free and pinned layers for a GMR structure containing top-pinned $a\text{-CoFeB}/\text{IrMn}$.

Here, we report the exchange bias from a top-pinned CoFeB/IrMn structure using an amorphous $\text{Co}_{40}\text{Fe}_{40}\text{B}_{20}$ layer. The antiparallel magnetic configuration between the free and pinned layers is proved by demonstrating a current-in-plane (CIP) GMR effect on simple Ru/CoFeB/Cu/CoFeB/IrMn/Ru stacks prior to and after annealing.

The Ru (5 nm)/CoFeB (3 nm)/Cu (2.5 nm)/CoFeB (3 nm)/IrMn (15 nm)/Ru (5 nm) thin film was deposited at room temperature on thermally oxidized silicon substrates by a dc magnetron sputtering system with a base pressure of better than 1×10^{-6} Pa. The deposition pressure was 5 mTorr. The deposition rates were about 0.1 nm/s for the Ru layer, 0.14 nm/s for the CoFeB layer, 0.09 nm/s for the Cu layer, and 0.17 nm/s for the IrMn layer. The compositions of the CoFeB and IrMn targets were $\text{Co}_{40}\text{Fe}_{40}\text{B}_{20}$ and $\text{Ir}_{22}\text{Mn}_{78}$, respectively. The as-deposited thin films were isothermally annealed at 280 °C for 1 h under a field of 5 kOe. The hysteresis loop was measured with a superconductor quantum interference detector. The MR was measured at a physical properties measurement system in a four-terminal geometry with a direct current of 1 mA. The microstructures were characterized using transmission electron microscopy (TEM) on Technai G2 F30 TEM.

^{a)}Electronic mail: c.y.you@nims.go.jp.

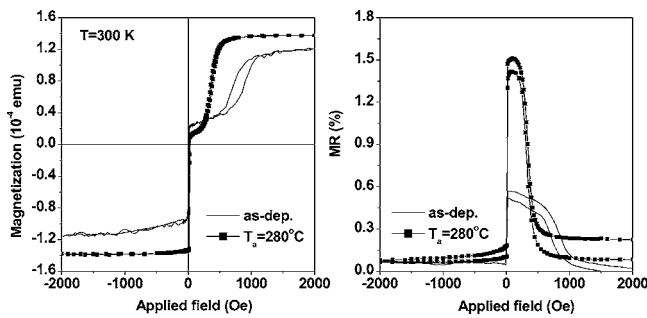


FIG. 1. Hysteresis loop and MR curve of the as-deposited and annealed samples measured at 300 K.

The exchange bias effect was checked and confirmed by fabricating a top-pinned CoFeB (10 nm)/IrMn (15 nm) bilayer thin film in the as-deposited and annealed states. Good crystalline and (111)-oriented texture structures of the IrMn layer have been obtained in the as-deposited state (data not shown here). In this work, we focus on the analyses of the spin valve structure of Ru (5 nm)/CoFeB (3 nm)/Cu (2.5 nm)/CoFeB (3 nm)/IrMn (15 nm)/Ru (5 nm). Figure 1 shows the hysteresis loop and the MR curve of the as-deposited and annealed samples measured at 300 K. The as-deposited sample has an exchange bias field of about 789 Oe higher than the annealed sample of about 375 Oe, which might be due to the short exchange coupled distance and smaller saturation magnetization of as-deposited sample. The stray field from cathode and interfacial uncompensated spins cause the appearance of exchange bias in the as-deposited state. A coercivity of less than 1 Oe was achieved for the free layer, which is beneficial for the sensitivity of the magnetic device. A significant MR increase from 0.5% to 1.4% was observed after annealing at 280 °C. The MR curve shows a plateau for the magnetization processes, indicating a large region of magnetic antiparallel configuration between the free and pinned layers. Figure 2 shows the low temperature hysteresis loop and the MR curve of the annealed sample at 5 K. The MR value significantly increased to 2.7%. The exchange bias field shows a slight enhancement to 442 Oe. Interestingly, the magnetic hysteresis of the pinned layer is significantly enhanced with a giant coercivity of 406 Oe. Due to a much bigger expansion of the magnetic hysteresis of the pinned layer, the magnetic antiparallel configuration between the free and pinned layers exists within a very narrow region when demagnetizing the sample from the exchange bias direction, showing a cusp in the MR curve marked by an arrow.

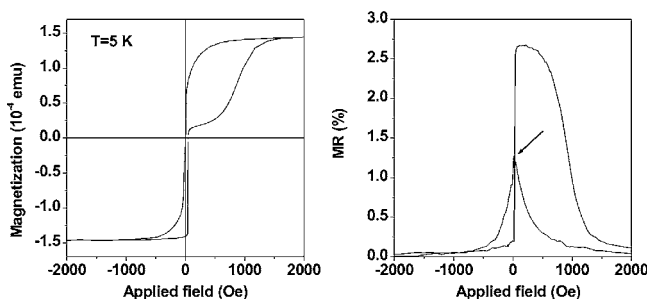


FIG. 2. Hysteresis loop and MR curve of the annealed sample measured at 5 K.

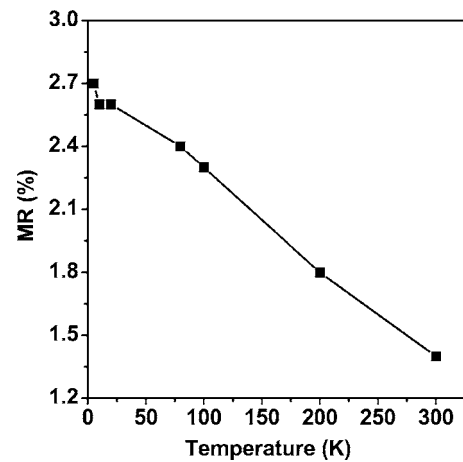


FIG. 3. Temperature dependence of MR of the annealed sample.

Figure 3 shows the temperature dependence of the MR value of the annealed sample. MR is enhanced significantly with decreasing measurement temperature. Approximately twice the MR is obtained when measured at 5 K compared to the measurement at 300 K. Another interesting aspect about the exchange bias is the comparison between the temperature dependences of the coercivities of the free and pinned layers. Figure 4 shows the temperature dependences of the coercivities of the free and pinned layers for the annealed sample. The coercivity of the pinned layer obviously has much higher temperature dependence than that of the free layer. The coercivity of the pinned layer shows an even bigger trend of coercivity enhancement below 50 K. In the free layer, the coercivity increases slightly with decreasing temperature, and then shows some higher enhancement below 50 K.

Figure 5(a) is the bright field image of the as-deposited sample, showing clear multilayered stacks. The bright field image of the annealed sample shown in Fig. 5(b), shows a more crystalline structure for all the layers. The top and bottom Ru layers consist of columnar grains. The crystallinity of the IrMn antiferromagnetic layer was further enhanced by

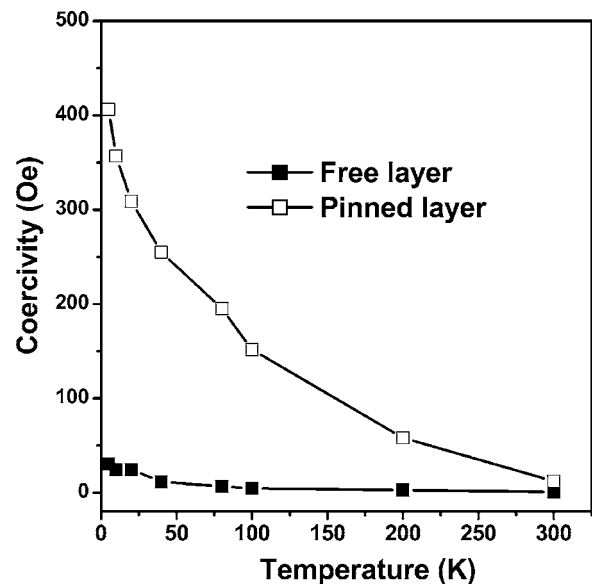


FIG. 4. Temperature dependence of the coercivities of the free layer and pinned layer of the annealed sample.

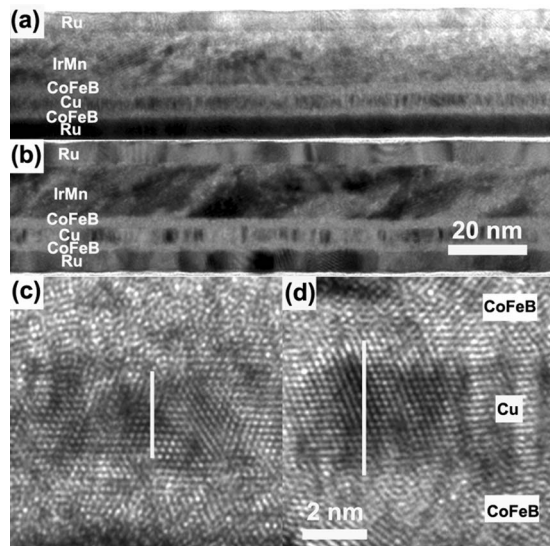


FIG. 5. Cross-sectional TEM images of [(a) and (c)] as-deposited and [(b) and (d)] annealed samples.

annealing. The Cu spacer layer exhibits a polycrystalline structure. Clear structural information can be seen from the high resolution TEM (HRTEM) images shown in Figs. 5(c) and 5(d). The HRTEM image of the as-deposited sample shows that the as-deposited CoFeB layer is clearly amorphous and the Cu spacer contains clear lattice fringes. After annealing, some of the CoFeB regions were crystallized showing the lattice fringe. By comparing the thicknesses of the crystalline regions within the Cu spacer before (~ 2.8 nm) and after annealing (4.2 nm), as indicated in the figures, the annealed sample is shown to have a wider crystalline region, implying that the CoFeB partially crystallized from the interface with Cu due to a better lattice matching between Cu and CoFe.

As reported in the references,^{14–17} the exchange bias has not been achieved from directly top-pinned structures of a - $\text{Co}_{72}\text{Fe}_8\text{B}_{20}$ or $\text{Co}_{60}\text{Fe}_{20}\text{B}_{20}/\text{IrMn}$ or FeMn at room temperature. However, inserting a thin fcc-NiFe layer was reported to result in the appearance of an exchange bias, which was explained by the improved crystalline and (111)-oriented texture structure of the antiferromagnetic IrMn or FeMn layer. Contrary to the references,^{14–17} the exchange bias was realized in the present work. The ordered antiferromagnetic IrMn is known to be a fcc structure. To minimize the surface energy, the close packed plane of (111) has to lie on the film plane in the absence of a large strain or distortions from the underlying layer. Therefore, if the underlying layer is fully amorphous, the crystalline IrMn with the (111) texture would develop spontaneously, as seen in this work. One possible reason for the no exchange bias in the references^{14–17} at room temperature might be due to the possible existence of some crystalline phases in the CoFeB layer, which would cause a random orientation of the subsequently deposited IrMn layer. Considering the compositions of $\text{Co}_{72}\text{Fe}_8\text{B}_{20}$ or $\text{Co}_{60}\text{Fe}_{20}\text{B}_{20}$ used in literatures,^{14–17} a less thermal stability of the amorphous structure of those alloys due to the higher Co content¹⁸ may result in a partially crystalline as-deposited CoFeB layer.

As shown in Fig. 4, the coercivity of the pinned layer is not only enhanced by the pinning effect from the IrMn layer, but also exhibits very high temperature dependence. There

are two different explanations for the coercivity enhancement by the pinning effects: induced anisotropy and the pinning sites of magnetic reversal from the antiferromagnetic layer.^{19,20} Here we cannot clarify which effect plays the main role in the coercivity enhancement. However, we can conclude that these effects are significantly dependent on temperature. One of the promising structural issues in this work is the observation of CoFeB partial crystallization from the interface with Cu, implying that a perfect interface between the Cu spacer and the ferromagnetic layer can be realized by postannealing, as seen in the CoFeB/MgO/CoFeB magnetic tunnel junction structure.

In summary, this work has shown that an exchange bias can be achieved from a directly top-pinned $\text{Co}_{40}\text{Fe}_{40}\text{B}_{20}/\text{IrMn}$ structure in the as-deposited state, in which CoFeB layer exhibits a fully amorphous structure. A CIP-GMR effect on simple Ru/CoFeB/Cu/CoFeB/IrMn/Ru stacks has been used to prove the feasibility to obtain the exchange bias from the top-pinned structure. By annealing, the CoFeB layer partially crystallizes from the interface with the Cu spacer layer, which would result in a better interface coherency between spacer and ferromagnetic layers. The coercivity of the pinned layer was found to have stronger temperature dependence than that of the free layer.

This work was in part supported by the Ministry of Education, Science, Sports and Culture, Grant-in-Aid for Scientific Research (B), No. 20360323, 2008 and the World Premier International Research Center Initiative (WPI Initiative) on Materials Nanoarchitectonics, MEXT, Japan.

¹Q. Yang, P. Holody, R. Loloee, L. L. Henry, W. P. Pratt, Jr., P. A. Schroeder, and J. Bass, *Phys. Rev. B* **51**, 3226 (1995).

²S. D. Steenwyk, S. Y. Hsu, R. Loloee, J. Bass, and W. P. Pratt, Jr., *J. Magn. Magn. Mater.* **170**, L1 (1997).

³M. Takagishi, K. Koi, M. Yoshikawa, T. Funayama, H. Iwasaki, and M. Sahashi, *IEEE Trans. Magn.* **38**, 2277 (2002).

⁴H. Fukuzawa, H. Yuasa, S. Hashimoto, K. Koi, H. Twasaki, M. Takagishi, Y. Tanaka, and M. Sahashi, *IEEE Trans. Magn.* **40**, 2236 (2004).

⁵H. Fukuzawa, H. Yuasa, K. Koi, H. Iwasaki, Y. Tanaka, Y. K. Takahashi, and K. Hono, *J. Appl. Phys.* **97**, 10C509 (2005).

⁶A. Jogo, K. Nagasaka, T. Ibusuki, A. Tanaka, and H. Oshima, *J. Magn. Magn. Mater.* **309**, 80 (2007).

⁷A. Jogo, K. Nagasaka, T. Ibusuki, H. Oshima, Y. Shimizu, T. Uzumaki, and A. Tanaka, *J. Magn. Magn. Mater.* **310**, 1895 (2007).

⁸S. Huang, E. Chen, and C. Chien, 52nd MMM Conference, 2007 (unpublished), ID No. CB-05.

⁹D. X. Wang, C. Nordam, J. M. Daughton, Z. H. Qian, and J. Fink, *IEEE Trans. Magn.* **40**, 2269 (2004).

¹⁰H. X. Wei, Q. H. Qin, M. Ma, R. Sharif, and X. F. Han, *J. Appl. Phys.* **101**, 09B501 (2007).

¹¹S. V. Karthik, A. Rajanikanth, Y. K. Takahashi, T. Ohkubo, and K. Hono, *Appl. Phys. Lett.* **89**, 052505 (2006).

¹²M. Jimbo, K. Komiyama, H. Matue, S. Tsunashima, and S. Uchiyama, *Jpn. J. Appl. Phys., Part 2* **34**, L112 (1995).

¹³M. Jimbo, K. Komiyama, and S. Tsunashima, *J. Appl. Phys.* **79**, 6237 (1996).

¹⁴M. Fujita, K. Yamano, A. Maeda, T. Tanuma, and M. Kume, *J. Appl. Phys.* **81**, 4909 (1997).

¹⁵T. Feng and J. R. Childress, *J. Appl. Phys.* **85**, 4937 (1999).

¹⁶S. Cardoso, C. Cavaco, R. Ferreira, L. Pereira, M. Rickart, P. P. Freitas, N. Franco, J. gouveia, and N. P. Barradas, *J. Appl. Phys.* **97**, 10C916 (2005).

¹⁷M. Fecioru-Morariu, G. Güntherodt, M. Rührig, A. Lamperti, and B. Tanner, *J. Appl. Phys.* **102**, 053911 (2007).

¹⁸X. Y. Mao, F. Xu, J. C. Tang, W. L. Gao, S. D. Li, and Y. W. Du, *J. Magn. Magn. Mater.* **288**, 106 (2005).

¹⁹H. Fujiwara, K. Nishioka, C. Hou, M. R. Parker, S. Gangopadhyay, and R. Metzger, *J. Appl. Phys.* **79**, 6286 (1996).

²⁰I. N. Krivorotov, T. Gredig, K. R. Nikolaev, A. M. Goldman, and E. Dan Dahlberg, *Phys. Rev. B* **65**, 180406 (2002).